JOURNAL OF THERMOPHYSICS AND HEAT TRANSFER
Vol. 8, No. 2, April–June 1994

Effects of Buoyancy on the Critical Heat Flux in Forced Convection

Matthew J. Brusstar* and Herman Merte Jr.†
University of Michigan, Ann Arbor, Michigan 48109

The critical heat flux (CHF) for R-113 was measured in forced convection over a flat surface at various orientations for relatively low flow velocities corresponding to Reynolds numbers ranging between 3000–6500 in the test section. As expected, the CHF was found to depend upon the orientation of the buoyancy. Although the buoyancy force acting on the vapor generally dominates over the flow inertia in this flow range, the inertia would continue to be substantial if the gravity was to be reduced significantly. In the experiments of this study, the CHF was determined for heating surface orientations ranging from 0 to 360 deg, for flow velocities between 4–35 cm/s, and for subcoolings between 2.8–22.2°C. The results presented here demonstrate the strong influence of buoyancy at low flow velocities, which diminishes as the flow velocity and subcooling are increased. In addition, a simple model in which the effects of varying the buoyancy orientation in pool boiling is incorporated is proposed to correlate the CHF at low flow velocities, which finally leads to an analogy between the CHF under adverse gravity and that under microgravity conditions.

Nomenclature

c_{pl} = specific heat of the liquid phase
F_{Buoy} = buoyancy force
F_{Drag} = drag force
g = gravitational acceleration
h_{fg} = latent heat of evaporation
L_c = characteristic length dimension
q_c = CHF
q_z = CHF in saturated pool boiling predicted by Zuber's model
q_{co} = q_z corrected for subcooling
U_t = terminal velocity of the vapor
ΔT_{sub} = subcooling
θ = orientation angle as designated in Fig. 5
ρ_l = density of liquid phase
ρ_v = density of vapor phase
σ = surface tension

Introduction

FUNDAMENTAL to studies in boiling is the critical heat flux (CHF), which represents the upper limit of the heat transfer obtainable through nucleate boiling under a given set of conditions. Whereas previous studies of the CHF have concentrated either on pool boiling or on forced convection boiling at relatively high flow velocities, little work has been devoted to the interval between these two extremes. In this intermediate region, with which this work is concerned, buoyancy dominates for the case near pool boiling, but its influence wanes with increasing flow velocity.

The study of flow boiling at low velocities finds application primarily in power generation and thermal management systems in space. The power consumption in such systems must be optimized with respect to the ability to transport heat effectively, and so the need arises for a greater understanding of forced convection boiling with reduced flow velocities. However, the knowledge gained thus far in investigations in this area under Earth's gravity applicable to microgravity is rather unsubstantial, due mainly to the difficulty in discerning the effects of the imposed velocity relative to buoyancy. Adding to this are the problems associated with obtaining microgravity or variable gravity for a sustained period of time in laboratory circumstances. The approach taken in the present work attempts to circumvent these problems by examining the effects of varying the orientation of the gravity vector with respect to the flow velocity. The magnitude and sign of the buoyancy force component in the direction of the imposed flow is therefore varied, along with the component normal to the flat heater surface used.

Several aspects of pool boiling are retained at relatively low flow velocities. The motion of the vapor is largely governed by buoyancy, and the flow inertia is rather inconsequential in determining the manner in which liquid is resupplied to the heating surface. In the case where the heating surface faces downward, vapor is pinned against the surface by buoyancy, which obstructs the return flow of liquid. A model is proposed which attempts to describe the CHF under such conditions. In this, the mechanisms for dryout may be compared to those which would be expected for flow boiling in microgravity, given the sliding motion of the void over the surface and the absence of hydrodynamic instabilities.

This study presents the results of the CHF measurements taken for a limited range of orientations, subcoolings, and flow velocities in forced convection boiling over flat, rectangular metal heating surfaces. A model which describes the effects of orientation on the CHF in subcooled pool boiling is compared with the results at low flow velocities, with reasonable agreement. As the effects of the flow inertia become more pronounced at the high velocity, however, it will be shown that the dependence of the CHF upon orientation changes significantly.

Model Description

The model presented here is an initial attempt to characterize the effects of varying the heating surface orientation on the CHF in pool boiling. Because of the many similarities of pool boiling and low velocity forced convection boiling,[1] it will be shown that the results of this model may be favorably compared with the experimental CHF data obtained at low velocities. The model is divided into two domains corresponding to upward-facing heating surface orientations and

Received Nov. 11, 1992; presented as Paper 93-0575 at the AIAA 31st Aerospace Sciences Meeting, Reno, NV, Jan. 11–14, 1993; revision received June 28, 1993; accepted for publication July 2, 1993.

*Graduate Research Assistant, Department of Mechanical Engineering and Applied Mechanics, 2250 G. G. Brown Laboratory.
†Professor of Mechanical Engineering, Department of Mechanical Engineering and Applied Mechanics, 2250 G. G. Brown Laboratory.

downward-facing ones, each of which is characterized by distinctly different mechanisms.

For upward-facing orientations, where buoyancy acts to carry the vapor away from the surface, vapor jet structures characteristic of the hydrodynamic instability models arise,[2,3] even in the presence of a relatively small forced flow tangent to the surface.[4] Under such strongly buoyancy-dominant conditions, the CHF in all upward-facing orientations may be approximated to a first-order by Zuber's model of the CHF over infinite, horizontal flat plates:

$$q_z = (\pi/24)\rho_v h_{fg}[\sigma g(\rho_l - \rho_v)/\rho_v^2]^{1/4} \quad (1)$$

The effects of subcooling may be incorporated based either on its influence on the rate of vapor condensation into the bulk liquid, or on the additional sensible energy necessary to heat the liquid from the subcooled to the saturated state. Correlations have been developed with reasonable success based on either premise, with both predicting a similar dependence on the Jacob number ($Ja = c_{pl}\Delta T/h_{fg}$). A correlation of the subcooling effect based on the latter premise is given by Ivey and Morris[5] as

$$q_{co} = q_z\left[1 + 0.102(\rho_l/\rho_v)^{0.75}\frac{c_{pl}\Delta T_{sub}}{h_{fg}}\right] \quad (2)$$

Values for the CHF of R-113 at various subcoolings based on Eq. (2) are plotted in Fig. 1.

For downward-facing orientations, a different CHF model must be constructed to account for the effects of adverse buoyancy on the processes of vapor removal and liquid replenishment at the surface. While previous studies of pool boiling[4] suggest the existence of jet-like vapor structures even on downward-facing surfaces, this seems unlikely in light of the tendency of the jets to collapse upon themselves under such conditions. In the present study, the vapor was observed to slide along the heating surface, pressed against it by buoyancy. A thin liquid layer could be seen evaporating on the heater surface, feeding the vapor mass hovering directly above the heater. Given these observations, an appropriate model of the CHF can be constructed based upon the obstruction of enthalpy flow to the surface caused by the sliding vapor mass. This concept is similar to that in the model presented by Weisman and Pei[6] for low-quality forced convection boiling, except that the motion at the surface is governed by buoyancy in the present case instead of by the flow inertia. As such, enthalpy is transported to the heating surface through entrainment behind the continuously departing vapor moving tangent to the surface, which effectively pumps the liquid from the bulk region into the thin film under the sliding vapor mass. Thus, it should be expected that the CHF will depend upon

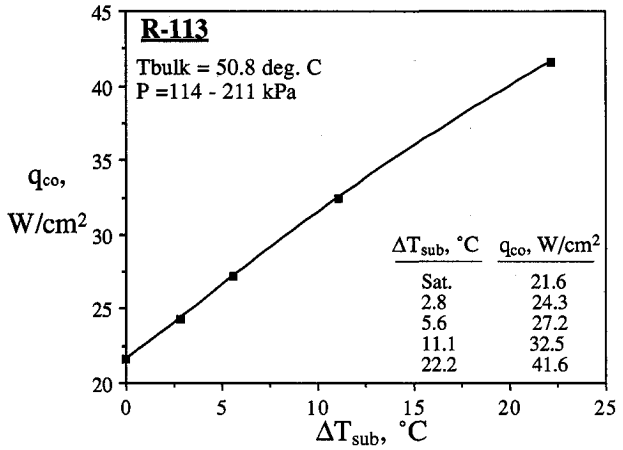

Fig. 1 CHF vs subcooling for R-113 in pool boiling over an infinite, horizontal flat plate.

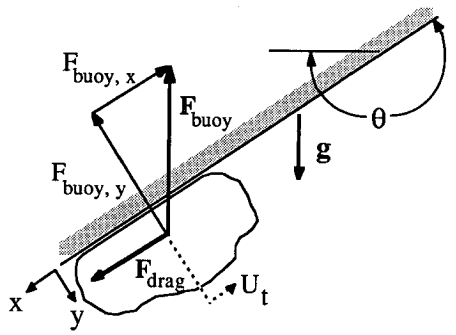

Fig. 2 Forces acting on a vapor mass under adverse buoyancy.

the velocity at which liquid is supplied to the surface, which may be approximated by the steady velocity of the departing vapor. Assuming the viscosity of the vapor to be small and that dryout occurs only at the CHF, such that the vapor slides along atop a thin liquid film, then viscous and solid-liquid-vapor surface tension effects can be neglected. The resulting balance of buoyancy and drag forces tangent to the heater surface (in the x direction), shown in Fig. 2, yields U_t, in Eq. (3):

$$\begin{aligned} F_{\text{Buoy},x} &= F_{\text{Drag}} \\ g\sin\theta(\rho_l - \rho_v)L_c^3 &\sim \rho_l U_t^2 L_c^2 \\ U_t &= \pm C|\sin\theta|^{1/2} \end{aligned} \quad (3)$$

where C is then a function of g, of some characteristic dimension for the vapor, and of the densities of the liquid and vapor. If it is assumed that the CHF varies continuously with orientation as the surface is rotated through the two vertical positions, 90 and 270 deg, then Eq. (2) establishes the boundary condition for the downward-facing domain. Using this, the predicted CHF for the downward-facing domain, from 90 to 270 deg, is given as

$$q_c = q_{co}|\sin\theta|^{1/2} \quad (4)$$

where q_{co} is defined by Eq. (2), and q_c is the CHF. This result, combined with that for upward-facing orientations, is compared below with experimental data.

Experimental Apparatus

The experiments were conducted in a forced convection loop shown schematically in Fig. 3. Generally, the loop provides for the controlled variation of four main parameters at the test section: 1) temperature, 2) subcooling, 3) flow velocity (or mass flux), and 4) orientation with respect to gravity. Automatic control schemes are utilized for maintaining the pressure, temperature, and flow velocity of the bulk liquid at the entrance of the test section at the desired levels. The entire loop can be rotated about its c.g., as shown, and fixed at any orientation between 0–360 deg. The salient features of the loop are described below.

R-113 flows through the loop at a set rate determined by the speed of a dc-driven centrifugal pump, which is controlled by an electrical feedback loop linked to a microprocessor. This arrangement provides the capability for varying the volume flow rate over a ratio of nearly 10:1, with a maximum output of approximately 7.5 l/min.

The pressure in the loop is maintained within about ±0.17 kPa of its set point by means of a pneumatically controlled stainless steel bellows. The set point is adjusted to provide the desired level of subcooling in the test section for the prescribed liquid temperature.

Two preheaters at the pump exit are used to raise the temperature of the R-113 at the inlet to the test section to the level desired, between 25–60°C. Preheater no. 1 raises the

bulk liquid temperature close to the desired level, while preheater no. 2 is then adjusted so that the measured inlet temperature reaches the desired value to within about ±0.06°C. Both preheaters receive hot water from a controlled constant-temperature reservoir at a flow rate varied by an electronic controller to obtain the desired test section inlet temperature, which is measured and fed back to the controller.

The test section is shown in greater detail in Fig. 4, and consists of a rectangular duct, 10.5 cm wide by 35.6 cm long. The height may be selected from three available sections to be 3.2, 12.7, or 25.4 mm, which permits varying the bulk velocity by more than a factor of 30 with the existing pump. Under maximum flow conditions, the Reynolds number based on hydraulic diameter for these test sections with R-113 is about 6500. On the sides and opposite the test surface are optical-grade quartz windows which allow for transverse as well as overhead views of the heater surface during operation.

A condenser-cooler following the test section acts to prevent cavitation at the pump inlet. Heat is removed from the loop through a counterflow shell-and-tube heat exchanger to a water-cooled reservoir. Cold water may also be circulated through the auxiliary condenser as necessary to aid in the removal of excess latent heat energy during CHF tests at low subcoolings.

The heater surface used for these experiments is shown in Fig. 5, and was designed to provide heat flux levels up to 80 W/cm^2. The heater consists of a copper body heated by three cartridge heaters in its base and insulated on all sides to provide a large heat capacity and uniformity of temperature at the boiling surface. Three chromel-constantan (type E) thermocouples are placed at precise locations beneath one another in the straight section leading to the upper surface so that the surface heat flux and temperature can be calculated. A smooth copper foil 0.1 mm thick was soldered over the top surface so as to prevent boiling at the crevices around the surface perimeter and in grooves on the surface produced by machining. The heating surface is rectangular in shape, 1.91 × 3.81 cm, and is flat so as to maintain a constant orientation between the body force and the heater surface. Additionally, the lack of curvature obviates any surface tension effects arising from varying wetting angles about the base of the bubbles forming on the surface.

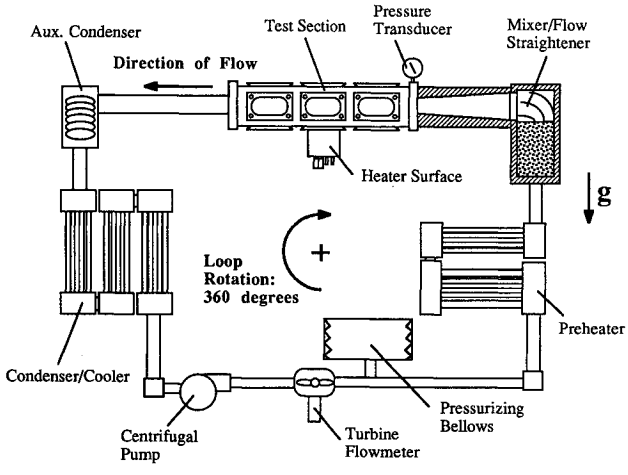

Fig. 3 Forced convection loop.

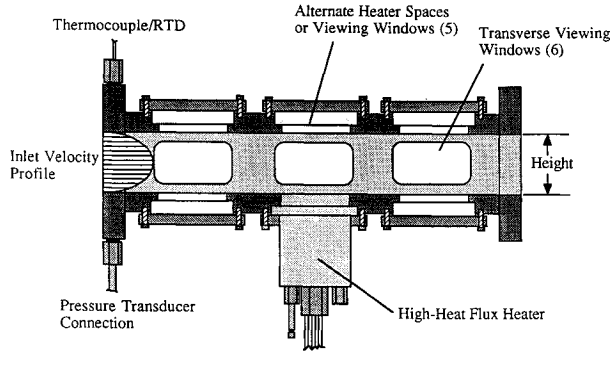

Fig. 4 Test section.

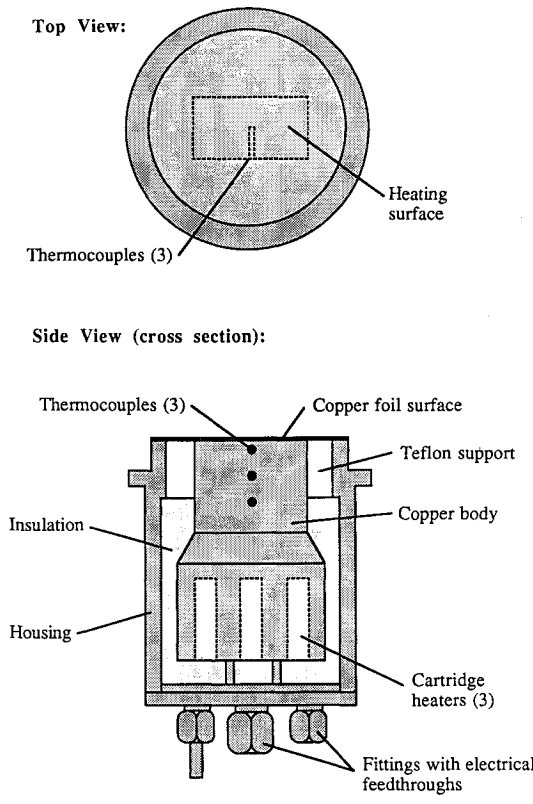

Fig. 5 High heat flux copper heater.

Before filling the flow loop, the R-113 is degassed and purified by filtering and distillation. The purity of the fluid was verified through measurements of the vapor pressure under quasisteady saturated conditions.

Experimental Procedures

Prior to installation in the flow loop, each test surface was calibrated in air to determine the heat lost to the surroundings as a function of the temperature at the base of the heater. Thus, the mean heat flux at the heater surface is determined by measuring the power input to the heater and subtracting the peripheral heat losses estimated from the measured base temperature. This yielded a more accurate estimate of the surface heat flux than that obtained from the measured temperature gradient in the heater. Although the two approximations generally compared rather favorably, the method employed here proved to be more consistent for cases such as the downward-facing orientations, where dryout occurred at isolated areas on the heating surface causing substantial variations in the heat flux over the surface.

The flow boiling experiments were conducted by first setting the orientation, flow velocity, pressure, and temperature in the loop to their desired values. Approximately 4 h were allowed for the loop to reach steady-state operating conditions before commencing testing. Nucleate boiling was initiated on the surface at a heat flux known to be far below the CHF as a precaution against a sudden jump into the film boiling region. Once quasisteady nucleate boiling had been attained, the voltage across the heater terminals was raised in an incremental fashion, allowing the surface to reach a quasisteady temperature at each step. The inlet temperature to the test section, the system pressure, the flow rate, the temperature measurements within the heater, and the input voltage and

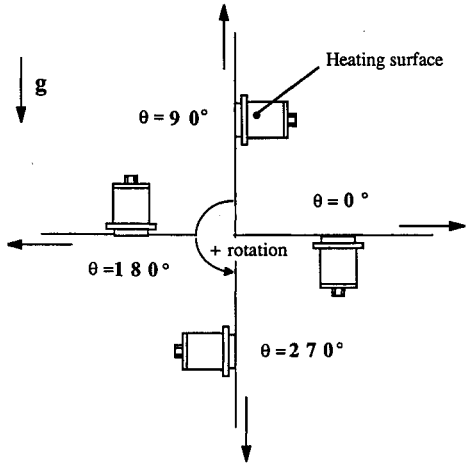

Fig. 6 Orientation angle designations. (Arrows indicate the direction of flow over the heating surface.)

current were then recorded before moving to the next higher increment.

The CHF was defined as that heat flux level above which a sudden or gradual temperature excursion at the heater surface was observed, which caused a safety relay to open the heater circuit. The last recorded quasisteady operating point prior to this event is subsequently used to calculate the CHF. All of the CHF measurements were repeated, some of them several times, to verify their reproducibility. The CHF measurements were quite reproducible, within a given uncertainty, although the accompanying surface superheat sometimes varied a few degrees, possibly as a result of changing nucleation patterns on the heater surfaces over time. The estimated uncertainties for some representative CHF measurements are given by the error bars in Figs. 7–9. Generally, the uncertainty in the measured CHF values was on average about ±8%, being somewhat greater for the smaller values and slightly less for the higher values of heat flux. In addition, some degree of subjectiveness is involved in the measurements of the very lowest CHF, occurring with the horizontal, downward-facing orientation at low flow velocities. In these cases, it was difficult to detect dryout of the heater surface, since the attendant temperature excursion was rather modest.

The various orientations used for these experiments are defined with respect to the horizontal upward position in Fig. 6. The flow direction over the heater surface is indicated by the arrows. Orientations intermediate to those shown are defined by the counterclockwise rotation. Vertical upflow corresponds to $\theta = 90$ deg, horizontal facing downward to $\theta = 180$ deg, and vertical downflow to $\theta = 270$ deg. The direction of the buoyancy force relative to both the imposed flow velocity and the heater surface changes with orientation, and is responsible for the effects to be demonstrated in the following section.

Results

Measurements of the CHF for R-113 with quasisteady heating are presented below for various orientations at different flow velocities and subcoolings. The effects of orientation on the CHF are considered first at low bulk velocities, where buoyancy is observed to dominate, as in pool boiling. A comparison of these data is then made with the results from the model discussed earlier, which includes the effect of subcooling. Measurements of the CHF for a higher flow velocity is then presented, which illustrates the effect of increasing flow momentum, as well as a dependence upon the void fraction resulting from the test section geometry.

Low Flow Velocities (4 and 8.5 cm/s)

Figure 7 shows the effect of orientation on the CHF, nondimensionalized with respect to the corresponding subcooled

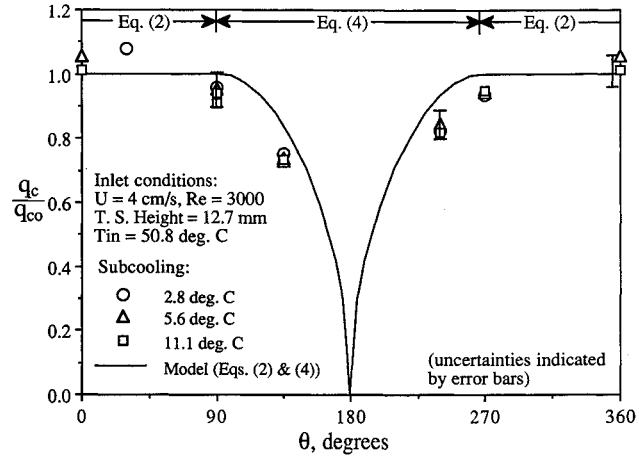

Fig. 7 CHF vs orientation angle, U = 4 cm/s.

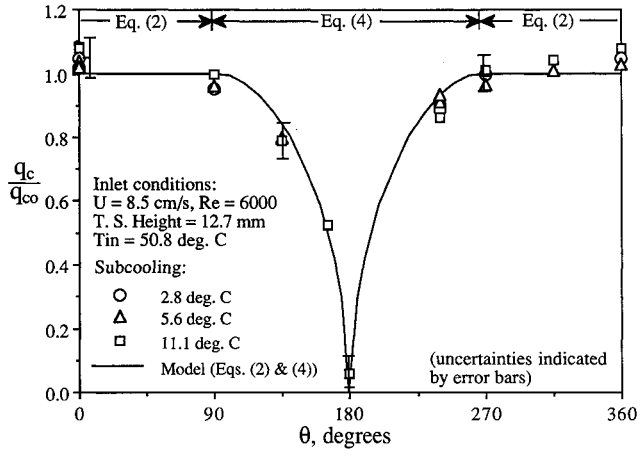

Fig. 8 CHF vs orientation angle, U = 8.5 cm/s.

pool boiling CHF values taken from Fig. 1, for a flow velocity of 4 cm/s. The test section inlet subcoolings were 2.8, 5.6, and 11.1°C. For the upward-facing orientations (θ = 0–90 deg, and 270–360 deg), the calculated CHF values agree reasonably well with the model. The strong dominance of buoyancy over the flow momentum is illustrated clearly with the downward-facing orientations (90 deg < θ < 270 deg), where the CHF decreases sharply to a minimum of nearly zero as the orientation approaches 180 deg. In this case, dryout of the heater surface was observed to occur at very near the onset of boiling, resulting from the inability of the imposed flow velocity to remove the vapor held against the heating surface by buoyancy. For all of the orientations at this flow velocity, the velocity of the vapor induced by buoyancy was observed to prevail over that of the bulk liquid flow.

The effect of subcooling at the low velocity, which is incorporated in the nondimensionalization, shows good agreement with the correlation expressed in Eq. (2) for both upward- and downward-facing orientations, although visual observations suggest different mechanisms for the influence of subcooling between these orientations. These observations are discussed later.

Figure 8 shows the CHF as a function of orientation for an imposed flow velocity of 8.5 cm/s. As in the previous figure, the data appear to agree well with the proposed model, indicating again the predominance of buoyancy relative to the inertia of the imposed flow at every orientation, including the horizontal facing downward position (180 deg). A comparison of the CHF for the upward-facing orientations with the pool boiling model shows only a modest increase, which may be attributable to the imposed flow. Perhaps more revealing, however, is a comparison of the CHF at the two vertical orientations, 90 and 270 deg, where upflow and downflow

exist, respectively. The two values are nearly identical, indicating very little effect associated with the flow inertia.

The effect of subcooling in Fig. 8 is similar to that observed in Fig. 7, and the data points are correlated very well, once again, by the model equation.

High Flow Velocity (35 cm/s)

Figure 9 shows the CHF for the highest velocity, 35 cm/s, nondimensionalized for subcoolings of 5.6, 11.1, and 22.2°C. Tests at lower subcoolings were not possible in the existing experimental facility due to the large amount of vapor generated at the heater surface, which interfered with the proper functioning of the flow loop. This high velocity was achieved by using the test section with the 3.2-mm height, which serves to increase the local void fraction for a given liquid velocity. The effect of the flow inertia is observed to be rather substantial, as the dramatic difference of the CHF values for vertical upflow (90 deg) and vertical downflow (270 deg) illustrate. Also, this figure differs strikingly from the two previous ones in that the minimum CHF is significantly greater than zero and occurs at a downward-facing orientation inclined with buoyancy against the direction of flow, at 240 deg. Also of note is the sag in the curve near 45 deg at the two lower subcoolings, which does not exist at the highest subcooling of 22.2°C. This effect is attributed to the small test section height, with the surface opposite the heater constraining the departing vapor. The data for the highest subcooling suggest that, in the absence of the large local void fraction brought about by the confining geometry, the maximum CHF for the lower subcoolings would also occur at an orientation of approximately 45 deg, where the surface is facing upward and is inclined with buoyancy acting in the direction of the flow.

Unlike the lower velocity cases of Figs. 7 and 8, the subcooling model used does not correlate the data well at the higher velocity of Fig. 9. The CHF decreases disproportionately as the subcooling is decreased, relative to the data presented in Figs. 7 and 8. Especially noteworthy in Fig. 9 is the behavior at $\theta = 45$ deg, where an increase in subcooling from 11.1 to 22.2°C increased the CHF to the same level as at $\theta = 0$ deg. It was observed that the void volume present above the heating surface at the highest subcooling was reduced notably from that at the lower subcoolings.

Discussion

Few studies relating to the effects of buoyancy on the CHF in forced convection exist with which the results of the previous section may be compared. However, as these data demonstrated, much of what was observed at the lower velocities is described well by pool boiling mechanisms. However, even for the case of pool boiling, the results with adverse buoyancy in particular require some interpretation.

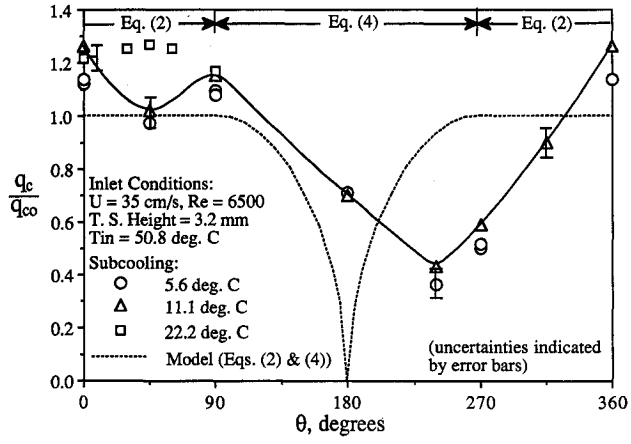

Fig. 9 CHF vs orientation angle, U = 35 cm/s.

The success of the hydrodynamic model exhibited at the low flow velocities is not surprising for the upward-facing orientations (0 deg $< \theta <$ 90 deg and 270 deg $< \theta <$ 360 deg), since the motion of the vapor departing the heating surface appeared to be largely unaffected by the imposed flow. For the downward-facing orientations (90 deg $< \theta <$ 270 deg), however, the vapor tended to slide over the surface, which thus lowered the CHF. This decrease may be attributed to several factors. First, the nearly static vapor mass existing above the heating surface under these conditions blocks much of the exchange of enthalpy with the bulk liquid region, and the CHF occurs upon dryout of the thin liquid layer remaining beneath the vapor at the surface. A similar mechanism for the CHF was noted previously by Tong and Hewitt[7] for flow boiling at low velocities and lower subcoolings, under conditions of slug flow. Secondly, the effect of excessive vapor production resulting from the increased contact area between the vapor and heated surface, and from thin film evaporation beneath the vapor tends to exacerbate the obstruction of the liquid inflow to the heater surface. This effect is reported in the work of Fujita et al.[8] for pool boiling, where the CHF is shown to decline substantially as the surface is rotated toward the horizontal facing downward position.

Previous measurements by other authors of the CHF at various orientations in pool boiling are nondimensionalized using Eq. (2) and compared with the proposed pool boiling model in Fig. 10. The widest discrepancy between the model and the data occurs in the horizontal downward-facing orientation (180 deg). In the preceding section, the actual measurements of the CHF at 180 deg with low flow velocities only slightly exceeded zero, as Fig. 8 indicates. The uncertainty in these measurements was very high, and the precise heat flux level where dryout of the surface occurred was difficult to detect. The CHF for downward-facing surfaces in pool boiling reported by Guo and El-Genk[9] and Ishigai et al.[10] for saturated water, and by Merte[11] for saturated LN_2 and LH_2, ranged from about 0.15–0.60 of the maximum CHF for upward-facing surfaces. In each of these cases, however, the experimental configurations permitted an escape path for the vapor about the heating surface periphery, which would give results higher than what would otherwise be expected for an infinite flat plate. Indeed, Ishigai et al. varied the size of the heating surface relative to the unheated peripheral area and found that the CHF decreased as the heating surface became proportionately smaller. The results of Vishnev et al.[12] for the steady heating of liquid He I agree well with the model at 180 deg, but not at other downward-facing orientations. Unfortunately, no details concerning the accuracy of these measurements are known.

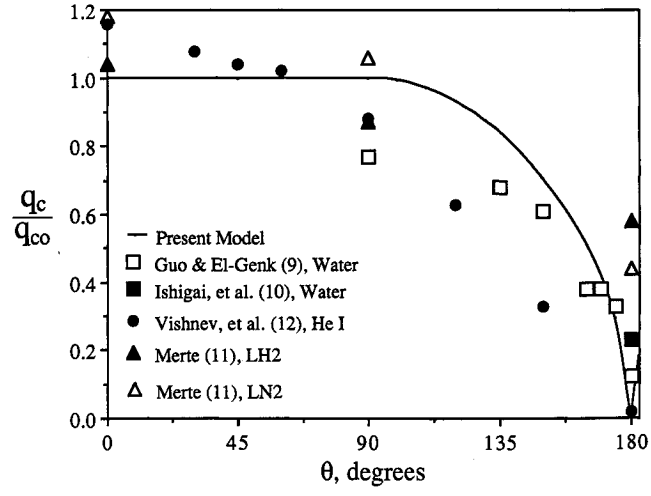

Fig. 10 Comparison of other CHF data with the proposed pool boiling model.

The effect of subcooling at low velocities is correlated fairly well by the model described earlier, although the physical means which produce this result likely differs between downward-facing and upward-facing orientations. Regardless of whether this effect is due to condensation of the departing vapor, as suggested by Zuber et al.,[13] or to the additional energy needed to bring the subcooled liquid to the saturated state,[14] the resulting correlation will take nearly the same form as Eq. (2). For downward-facing orientations, where the CHF results upon dryout of a liquid film, the subcooling effect will be like that described by Kutateladze, whereas for the CHF with upward-facing orientations (0 deg $< \theta <$ 90 deg and 270 deg $< \theta <$ 360 deg), which results from hydrodynamic instability, condensation likely is the predominant effect.

The effect of flow velocity in Figs. 7 and 8 is rather small, owing to the fact that the buoyant velocity was predominant over that of the imposed flow. As the flow inertia was increased, however, Fig. 9 shows that there results a significant departure from the near-pool boiling behavior exhibited in the two previous figures. While the vapor was still observed to slide along the surface for the downward-facing orientations at the high flow velocity, its motion was markedly influenced by the forced flow. As a result, the CHF at the high velocity was not so dramatically affected by the adverse buoyancy of the horizontal downward position (180 deg), even though a general decreasing trend in the data is seen for downward-facing orientations. Papell[15] studied the relative effects of buoyancy and flow momentum by comparing the CHF in vertical tubes for the cases of upflow and downflow. The results presented were divided into buoyancy-dependent and buoyancy-independent flow regimes, which were functions of the flow velocity, subcooling, and system pressure. The dependence upon buoyancy was said to have been brought about by an accumulation of void resulting from the balance of buoyancy and drag forces, an effect which was mitigated as the flow inertia was increased. An earlier visual study by Simoneau and Simon[16] in a similar configuration affirms these assertions. A comparison of the two vertical orientations, θ = 90 and 270 deg, in Fig. 9, also exhibits the same phenomenon. Indeed, visual observations at the CHF with downflow showed a congregation of vapor bubbles above the surface as a result of the near balance of inertia and buoyancy forces, which consequently resulted in a lower CHF.

The influence of subcooling in Fig. 9 appears to be more complex than that for the lower flow velocities, as witnessed by the relatively poor correlation of the data with Eq. (2). The difference in this case is that the CHF was adversely affected by the large void volume produced by the heater, which increases with decreasing subcooling. This effect is compounded by the relatively narrow test section height (3.2 mm) used for the high velocity experiments. The most striking example of this occurs at θ = 45 deg, where the decrease in the CHF between 0–90 deg at lower subcoolings disappears as the subcooling is raised to 22.2°C. A similar effect of void fraction was noted by Papell[15] and Simoneau and Simon[16] in the works cited above, where an increase in subcooling decreased the accumulation of void near the surface, which thereby reduced the adverse effects on the CHF associated with downflow.

In the downward-facing orientations, where the departing vapor is observed to slide along the surface, and where there is an absence of unstable hydrodynamic phenomena, an analogy with forced convection in microgravity. In pool boiling in microgravity, it was observed by Ervin[17] that the vapor remains stationary upon the heating surface following the onset of boiling. In the presence of an imposed liquid flow, it may be expected that the vapor would slide along the surface, and that the mechanism for the CHF would be the evaporation of the thin liquid film existing beneath the vapor. Under conditions of adverse buoyancy, the same mechanism dominates, much as if conditions of slug flow prevailed. The heat flux at which dryout of the film occurs depends on the rate at which the film is replenished, and on the subcooling of the incoming liquid. The film thickness is deduced to be independent of buoyancy,[18] so that the motion of the vapor, whether driven by the inertia of the imposed flow or by buoyancy, will determine the rate at which the film is replenished, and thus will govern the CHF. In this way, the mechanism of the CHF for downward-facing orientations under Earth's gravity could be viewed as similar to that which would exist with forced convection boiling in microgravity. For example, in the case where there is no motion of the vapor at the heating surface, as with the horizontal down position at low flow velocities and with pool boiling in microgravity, the data presented here and by Ervin show that the CHF occurs at levels approaching zero. When buoyancy induces motion of the departing vapor, as predicted by Eq. (3), the CHF then rises in a manner which may be described by mechanisms similar to those for forced convection in microgravity.

Conclusions

1) Buoyancy dominates the CHF mechanisms at low flow velocities, much as in pool boiling. The role that the forced flow inertia would otherwise play in the absence of gravity is thus obscured, and it is seen to have only a modest effect on the CHF in the presence of Earth's gravity.

2) Except in cases of excessive void fraction, as observed in the experiments at the high velocity, the effects of subcooling may be attributed to the increased contribution of sensible heat energy. A correlation based on this assumption was used with good success.

3) The CHF at downward-facing orientations seems to be determined mainly by the rate at which liquid is fed to the heating surface by means of entrainment behind the departing vapor. An analogy can be drawn between this condition and that which would exist in forced convection boiling in microgravity.

Acknowledgment

This work was supported in part under NASA Grant NAG3-589.

References

[1]Katto, Y., "Critical Heat Flux," *Advances in Heat Transfer*, Vol. 17, 1985, pp. 1–64.

[2]Zuber, N., "On the Stability of Boiling Heat Transfer," *Transactions of the American Society of Mechanical Engineers, Series C, Journal of Heat Transfer*, Vol. 80, No. 4, 1958, pp. 711–720.

[3]Lienhard, J. H., and Dhir, V. K., "Hydrodynamic Prediction of Peak Pool-Boiling Heat Fluxes from Finite Bodies," *Transactions of the American Society of Mechanical Engineers, Series C, Journal of Heat Transfer*, Vol. 95, No. 2, 1973, pp. 152–158.

[4]Haramura, Y., and Katto, Y., "A New Hydrodynamic Model of Critical Heat Flux, Applicable to Both Pool and Forced Convection Boiling on Submerged Bodies in Saturated Liquids," *International Journal of Heat and Mass Transfer*, Vol. 26, No. 3, 1983, pp. 389–399.

[5]Ivey, H. J., and Morris, D. J., "On the Relevance of the Vapour-Liquid Exchange Mechanism for Subcooled Boiling Heat Transfer at High Pressure," UKAEA, AEEW-R 137, 1962.

[6]Weisman, J., and Pei, B. S., "Prediction of the Critical Heat Flux in Flow Boiling at Low Qualities," *International Journal of Heat and Mass Transfer*, Vol. 26, No. 10, 1983, pp. 1463–1477.

[7]Tong, L. S., and Hewitt, G. F., "Overall Viewpoint of Flow Boiling CHF Mechanisms," American Society of Mechanical Engineers Paper 72-HT-54, 1972.

[8]Fujita, Y., Ohta, H., Uchida, S., and Nishikawa, K., "Nucleate Boiling Heat Transfer and Critical Heat Flux in Narrow Space Between Rectangular Surfaces," *International Journal of Heat and Mass Transfer*, Vol. 31, No. 2, 1988, pp. 229–239.

[9]Guo, Z., and El-Genk, M. S., "An Experimental Study of Saturated Pool Boiling from Downward Facing and Inclined Surfaces," *International Journal of Heat and Mass Transfer*, Vol. 35, No. 9, 1992, pp. 2109–2117.

[10]Ishigai, S., Inoue, K., Kiwaki, Z., and Inai, T., "Boiling Heat Transfer from a Flat Surface Facing Downward," *International De-*

velopments in Heat Transfer: Proceedings of the 1961 Heat Transfer Conference, 1961, Paper 26, pp. 224–229.

[11]Merte, H., Jr., "Nucleate Pool Boiling in Variable Gravity," Vol. 30, Progress in Astronautics and Aeronautics, AIAA, Washington, DC, 1990, pp. 15–69.

[12]Vishnev, I. P., Filatov, I. A., Vinokur, Ya. G., Gorokhov, V. V., and Svalov, G. G., "Study of Heat Transfer in Boiling of Helium on Surfaces with Various Orientations," *Heat Transfer—Soviet Research*, Vol. 8, No. 4, 1976, pp. 104–108.

[13]Zuber, N., Tribus, M., and Westwater, J. W., "The Hydrodynamic Crisis in Pool Boiling of Saturated and Subcooled Liquids," *International Developments in Heat Transfer: Proceedings of the 1961 Heat Transfer Conference*, 1961, Paper 27, pp. 230–236.

[14]Kutateladze, S. S., *Fundamentals in Heat Transfer*, Arnold, London, 1963, p. 387.

[15]Papell, S. S., "Buoyancy Effects on Forced-Convective Boiling," American Society of Mechanical Engineers Rept. 67-HT-63, 1967.

[16]Simoneau, R. J., and Simon, F. F., "A Visual Study of Velocity and Buoyancy Effects on Boiling Nitrogen," NASA TN D-3354, 1966.

[17]Ervin, J. S., "Incipient Boiling in Microgravity," Ph.D. Dissertation, Dept. of Mechanical Engineering, Univ. of Michigan, Ann Arbor, MI, 1991.

[18]Bankoff, S. G., "Dynamics and Stability of Thin Heated Liquid Films," *Journal of Heat Transfer*, Vol. 112, No. 3, 1990, pp. 538–546.